04

Reducing the effect of external magnetic fields on the operation of a gas-filled neutron tube

© I.M. Mamedov,[1,2] S.P. Maslennikov,[1,2] A.A. Solodovnikov,[3] A.Yu. Presnyakov[1]

[1]Dukhov All-Russia Research Institute of Automatics,
127055 Moscow, Russia
[2]National Research Nuclear University „MEPhI"
115409 Moscow, Russia
[3]Moscow Institute of Physics and Technology (State University),
117303 Moscow, Russia
e-mail: schildkrote5552@yandex.ru

Received August 8, 2023
Revised August 7, 2024
Accepted August 16, 2024

The results of studies of the operating modes of ion Penning sources in the composition of small-sized gas-filled neutron tubes under the influence of external magnetic fields arising during the operation of logging equipment due to the intrinsic magnetization of casing strings are presented. According to the research results, it is shown that the greatest negative effect on the operation of neutron generators is exerted by a transversely directed external magnetic field. Based on the data obtained, options for constructing a shielded magnetic neutron tube system are proposed, taking into account the design features of the generator elements and the robust housing of the well geophysical research equipment. Measurements of the pressure dependences of the amplitude and delay of the pulse for shielded Penning ion sources have confirmed their effectiveness in improving the stability of neutron generators.

Keywords: Penning ion source, gas-filled neutron tube, pulsed neutron generator, well-logging equipment.

DOI: 10.61011/TP.2024.10.59356.138-24

Introduction

Small-sized gas-filled neutron tubes (GNTs) are used widely in pulsed neutron generators (PNGs), which are the essential components of equipment for well logging, non-destructive testing, nuclear medicine, etc. [1]. Penning ion sources (PISs), which are characterized by a simple design and a wide range of adjustment of operating parameters, are often used as sources of accelerated ions of hydrogen isotopes in neutron tubes of this type. The regimes of discharge in crossed electric and magnetic fields depend on the gas composition and pressure, the geometric parameters and the voltage at the electrode system of a discharge cell, and the strength and spatial distribution of the magnetic field [2]. Although PISs have long been studied and applied in practice [3–19], a comprehensive physical model characterizing the entire complex of processes of Penning discharge generation and formation of ion fluxes have not been developed yet. This is the reason why experimental research and optimization of PIS operating regimes in the actual operation environment of neutron equipment, which have a direct influence on its stability and long-term performance, remains relevant.

GNT-based equipment for spectrometric pulsed neutron-gamma logging of oil wells with casing strings has been designed at the Dukhov All-Russia Research Institute of Automatics and is being mass-produced at present [20,21]. The obtained research data demonstrated that a common cause of disruption of stable operation of neutron generators is the influence of external magnetic fields. In a well, the likely sources of magnetic fields with their strength reaching hundreds of gauss are the magnetization of a casing string and anomalies of magnetic fields in pipe couplings [22,23].

In the present study, we report the results of experimental studies into the operating regimes of PISs affected by external magnetic fields, which provided an opportunity to construct shielded magnetic GNT systems for well-logging equipment with account for the design features of the PNG emitter unit.

1. Formulation of the problem and experimental methods

The studies of Penning discharge cells used in equipment of various functions revealed several discharge modes and regimes [2–3,24–27]. Each of these modes is observed at certain geometric parameters of the electrode system, composition and pressure of the working gas, spatial distribution and strength of the magnetic field, and operating regime of the power supply system. The following discharge modes were identified by analyzing the results reported in [2–3]: Townsend regime, weak magnetic field regime, strong magnetic field regime, transient regime, high-pressure regime, and glow discharge regime. The following three characteristic types of discharge regimes

were proposed in [27]: high-voltage low-pressure discharge ($P \leq 10^{-4}$ Torr); transient discharge form within the intermediate pressure range ($P \sim 10^4 \cdot 10^{-3}$ Torr); and glow reflective discharge at elevated pressures ($P \gg 10^{-3}$ Torr). The specified boundaries of pressure ranges are not fixed and depend on the magnetic field strength, the anode voltage, and the geometric parameters of the discharge cell.

The transition of a discharge from one mode to another is accompanied by changes in the conditions of discharge initiation, the distribution of the spatial charge density and the potential in the interelectrode gap, and discharge current and voltage. In the context of PISs, the efficiency of extraction of ion fluxes, their amplitude characteristics, and the discharge ignition delay vary from one discharge mode to the other.

The results of examination of a Penning discharge for vacuum gauges and ion pumps were summarized in [2,3,24–26]. It was found that the dependences of the discharge current on magnetic field have a complex and non-monotonic form. In the region of weak magnetic fields, an increase in field strength is accompanied by a virtually linear growth of discharge current. When the field strength exceeds a certain threshold value, the current stops growing and starts to decrease, eventually reaching a certain steady level. In the region of strong magnetic fields, the discharge current depends only weakly on the field strength.

It was demonstrated in [28–30] that the configuration of the magnetic field applied to a Penning discharge cell in PISs of small-sized neutron tubes has a significant influence on the discharge mode and on the amplitude-time characteristics (ATCs) of generated ion fluxes. The obtained results were analyzed, and it was proposed to use a non-uniform magnetic field distribution in PISs with the axial field induction component decreasing linearly by 10−15% within the cell length toward the extracting electrode.

Experimental dependences of the discharge and extracted currents on the magnetic field strength for various types of PISs used in GNTs were presented in [31–33]. It should be noted that the discharge and extracted currents were maximized at different magnetic field strengths. In view of this, one needs to take into account the redistribution of currents, operating voltages, and power consumption of the device when examining the ways to increase the efficiency of PIS operation.

The present study is focused on small-sized GNTs designed for application in well-logging equipment. A GNT is a compact linear accelerator of deuterium ions transported to a neutron-producing target. All tube elements (ion source, ion-optical system, and target unit) are assembled in a sealed housing. A PIS features a cylindrical anode coaxial with two disk cathodes that are positioned in an axial magnetic field. The accelerating electrode and the neutron-producing target, which are under a high negative potential, are isolated galvanically from the PIS with a high-voltage insulator. The studied PIS and GNT were discussed in detail in [22–23,28].

2. Experimental equipment and measurement procedure

Test GNT units were connected via an exhaust tube to the vacuum system of the experimental stand fitted with a set of sensors for online measurement of pulsed voltages at the anode of the ion source, pulsed currents in the anode and cathode branches of the ion source, the bias voltage, and the extracted pulsed current at the target [28,29,34]. The maximum residual pressure was $1 \cdot 10^{-6}$ Torr. A built-in getter (working gas storage) was used to fill the GNT volume with working gas (deuterium) and regulate its pressure within the 0.1−10 mTorr range. An axially symmetric magnetic field of varying magnitude and configuration was produced in the PIS using a cylindrical current coil or assemblies of several ring magnets. The conditions for discharge ignition in magnetic fields with a non-uniform distribution were simulated by shifting the current coil along the system axis [28,29]. The parameters of pulses to the anode in the pulse-periodic power supply regime were as follows. The repetition rate of supply voltage pulses was set either to $f = 600$ Hz with pulse duration $t_{vp} = 200\,\mu$s or to $f = 10$ kHz with $t_{vp} = 30\,\mu$s. The anode voltage amplitude (U_a) was adjusted within the 1.5–3.0 kV range.

In experiments where the studied GNT was not immersed in transformer oil, the accelerating voltage applied to the target electrode of the tube was $U_{ex} = -20$ kV. The studies of operating regimes of pulsed neutron generators performed in [9,19] revealed a direct connection between the shape of a current pulse at the target and the shape of a neutron burst. A linear relation between the current extracted from the PIS and the neutron flux (at different levels of accelerating voltage) was demonstrated in [35] for the GNT type under study. It was also demonstrated in [36,37,38] by independent methods that virtually the entire ion beam extracted from the PIS reached the target in the examined GNT geometry under accelerating voltages $U_{ex} \geq 20$ kV. Direct measurements of the beam profile at the target under a negative potential [39] demonstrated that the spot diameter did not increase at accelerating voltages above 20 kV in the geometry of the ion-optical system used in the GNT examined here.

3. Results and discussion

The dependences of the discharge and extracted currents on pressure in the pulsed power supply regime of operation of ion sources were determined in a series of experiments with several test neutron tubes. Experiments were performed at various parameters of the magnetic system of ion sources. Both the strength of the magnetic field (produced by permanent magnets) in the ion source and the distribution structure (configuration) of this field were varied.

3.1. Influence of external magnetic fields on the GNT operation

The results of studies on identifying the optimal magnetic field configuration in the GNT PIS providing the shortest discharge ignition times with maximum values of the extraction coefficient (the ratio of the ion current extracted from the PIS to the discharge current) were reported in [28–31]. Operational experience with neutron generators suggests that studies into the influence of external sources of magnetic fields on the operation regimes of PISs found in small-sized GNTs are practically relevant.

This served as a starting point for further research aimed at improving the stability of operation of neutron tubes in external magnetic fields produced by magnetized wellbore elements or external objects in the vicinity of a neutron generator. This research was carried out on the assumption that the equipment of interest is exposed to an asymmetric lateral external magnetic field with a strength of about 100 G, which is consistent with the actual well logging conditions [22].

Test GNTs were installed in the tube unit (TU) and the emitter unit (EU) of real pulsed neutron generators. Figure 1 shows the distribution pattern of self-magnetic fields in the ion source region obtained via modeling in Comsol Multiphysics. Calculations were carried out for the parameters of magnets that are used in actual equipment and fit its operating conditions in terms of temperature stability, neutron tolerance, dimensions, etc.

The presented data visualize the structure of the magnetic field and its homogeneity inside the PIS; the magnetic field lines allow one to determine the ratio of longitudinal and transverse field components, which has a decisive influence on the operating regimes of the neutron tube [29]. In subsequent experiments, control measurements of the distribution of the axial field component on the PIS axis

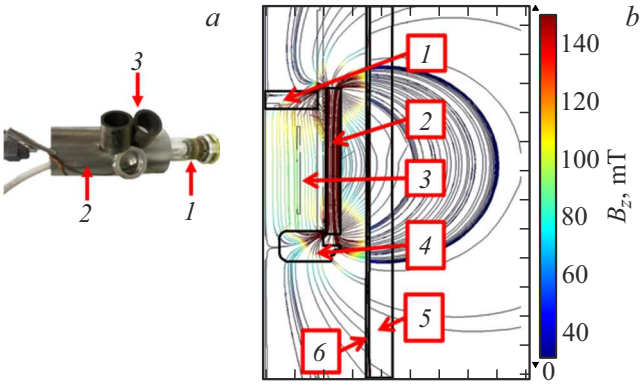

Figure 1. *a* — Photographic image of the GNT (*1*) with a housing imitating TU and EU (*2*) and external „parasitic“ magnets (*3*); *b* — magnetic field distribution in the PNG near the GNT (calculated in Comsol Multiphysics), *1* — PIS cathode (kovar), *2* — permanent magnets, *3* — PIS anode (stainless steel), *4* — PIS anti-cathode (kovar), *5* — EU (stainless steel), and *6* — TU (AISI 1008 steel).

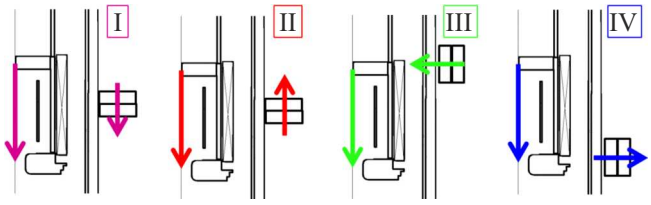

Figure 2. Different arrangements of external magnets in the vicinity of the ion source.

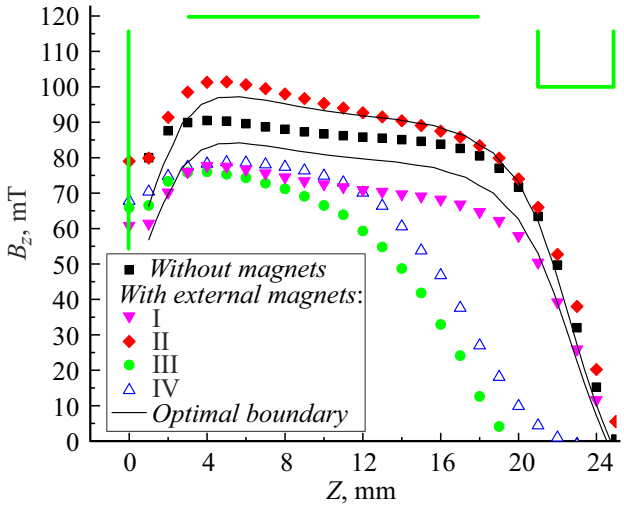

Figure 3. Distribution of the magnetic field inside the GNT PIS with external magnets installed. The coloring scheme is the same as in Fig. 2.

were carried out with the use of Hall sensors introduced into the discharge cell through an aperture in the anti-cathode.

Several series of experiments were conducted with different arrangements of external „disturbing“ magnets relative to the PIS. NdFeB magnetic assemblies $30 \times 20 \times 25$ mm in size with a magnetic field strength at their end surface of ~ 0.4 T were used. These assemblies produced an external magnetic field in the PIS region consistent with the operating conditions of well-logging equipment [22].

The results of examination of ignition regimes and characteristics of a Penning discharge for four different arrangements of external magnets in the vicinity of the ion source (Fig. 2) are reported below. Arrangements I and II correspond to such conditions when the external magnet was positioned in the central PIS part to produce a magnetic field contra- or co-directional with the field inside the PIS. Options III and IV: the external magnet is located in the region of the cathode and the anti-cathode to produce a transverse external magnetic field.

Figure 3 shows the $B_z(z)$ dependences plotted based on the results of on-axis measurements of the magnetic field (individual points) produced by the intrinsic magnetic system without external disturbing influences and with external magnets arranged in different ways. Solid curves

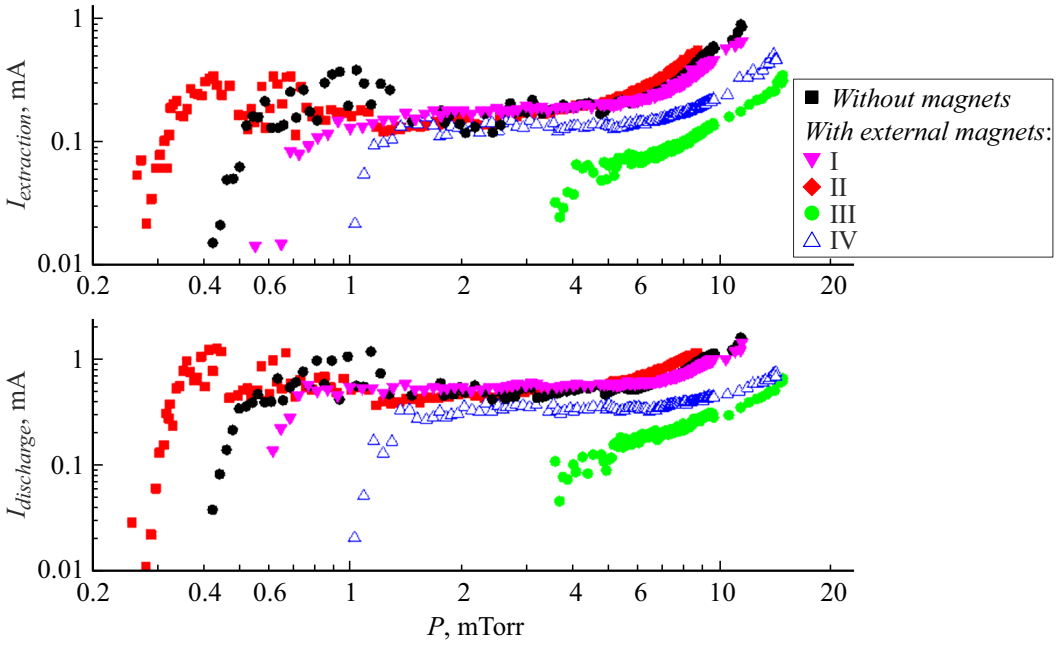

Figure 4. Dependence of discharge current I_d and extracted current I_{ex} on pressure without and with an external magnetic field.

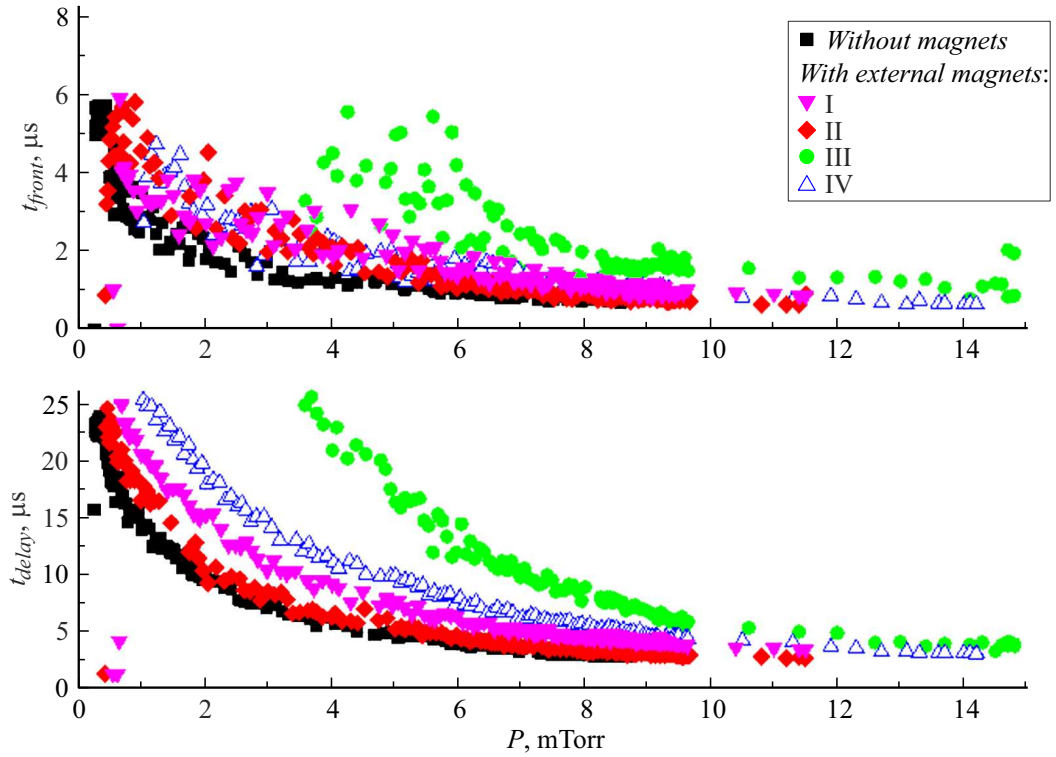

Figure 5. Dependence of delay time t_{delay} and front time t_{front} on pressure without and with an external magnetic field.

indicate the range of optimal distribution of the magnetic field in the discharge cell that ensures stable PIS operation.

The presented data demonstrate clearly that the magnetic field may vary both upward and downward depending on the direction of magnetization of the external source. When the external field is directed transversely, the $B_z(z)$ distribution is deformed.

Figures 4 and 5 present the results of experiments on measuring the dependences of the amplitude parameters of discharge and extracted currents and the delay and rise times

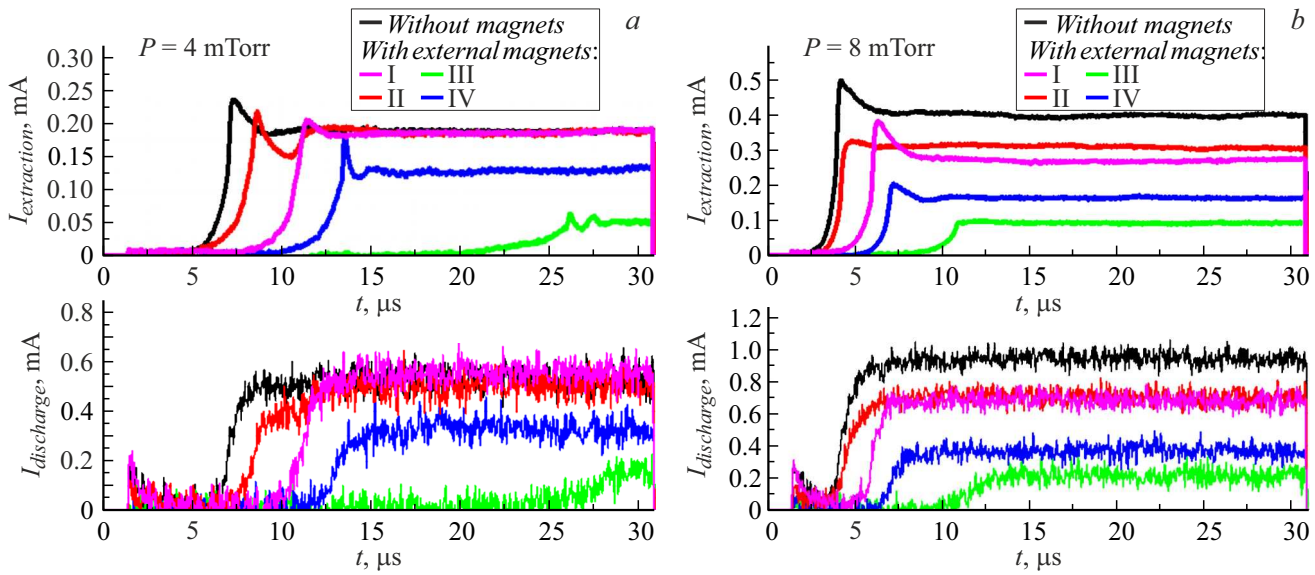

Figure 6. Characteristic oscilloscope records of discharge current and extracted current without and with an external magnetic field at different working gas pressures P: a — 4, b — 8 mTorr.

of discharge current pulses on the working gas pressure in the PIS with the neutron tube operating in different magnetic environments: without external sources and with external magnets arranged in four different ways.

The dependences of the amplitude values of discharge current I_d and extracted current I_{ex} on pressure (Fig. 4) were investigated within the range of $P = 0.3-15$ mTorr where stable discharge ignition was observed.

Figure 5 shows the dependences of discharge ignition delay t_{delay} and front time t_{front} of the discharge current on pressure. It can be seen from Figs. 4 and 5 that the discharge current amplitude decreased by 30–35% when external magnets were present, while the discharge ignition delay increased by $2-4\,\mu$s (from $t_{delay} \approx 6\,\mu$s to $\approx 8-10\,\mu$s). In the experiment with a transverse external field in the cathode region, discharge ignition was not observed at pressures below 4 mTorr, a nearly fourfold reduction in amplitude of the discharge current was noted, and the discharge ignition delay exceeded $15\,\mu$s.

The obtained results suggests that the housing of a logging instrument made of stainless steel 12Kh18N10T does not suppress the influence of magnetized materials located in the immediate vicinity of the PNG emitter. The field of external magnets disrupts the field structure in the PIS (Fig. 4), potentially leading to failure. Notably, the negative influence of an external magnetic field is the most profound and leads to significant degradation of PIS performance when the external magnetic field in the cathode region is transverse to the PIS axis. It can be seen from Figs. 4 and 5 (magnet arrangement III) that the discharge was ignited at elevated pressures ($P \geq 4$ mTorr) and the current amplitudes decreased by a factor of more than 2.

Figure 6 presents the pulse shapes of discharge and extracted currents in the PIS operating without disturbing magnetic influences and with external magnets arranged in four different ways. The operating parameters of the power supply system remained unchanged: $U_a = 2$ kV, $t_{vp} = 30\,\mu$s, and $f = 10$ kHz. Measurements of the discharge characteristics were carried out at two values of the working gas pressure in the discharge cell: $P = 4$ mTorr (Fig. 6, a) and $P = 8$ mTorr (Fig. 6, b). The obtained data demonstrate that the conditions for discharge ignition in the examined ion source design (without magnetic shielding) are violated at any position of the external magnet. The shape of pulsed currents, their amplitude parameters, and the discharge ignition delay are all altered.

As for pulsed ion currents recorded at the target, their amplitude decreases, and the time needed to form an ion flux increases significantly. These are the signs of disturbance of neutron flux generation regimes. The strongest impact on the operating conditions of the ion source was noted in the case of a transverse external magnetic influence in the cathode region. Specifically, at pressure $P = 4$ mTorr, an ion pulse at the target forms with a delay of approximately $25\,\mu$s, and the pulsed current amplitude decreases by a factor of almost $\sim 3-4$ relative to the one measured in unperturbed operation of the ion source.

3.2. Shielded magnetic PIS systems

Additional magnetic screens enveloping the PIS may be used to suppress the influence of external magnetic field sources on the operating regimes of the neutron tube. Since the external dimensions of well-logging equipment are rather small, shielding elements are located in close proximity to the magnetic system of the neutron tube (the permissible gap width is approximately 3 mm) and,

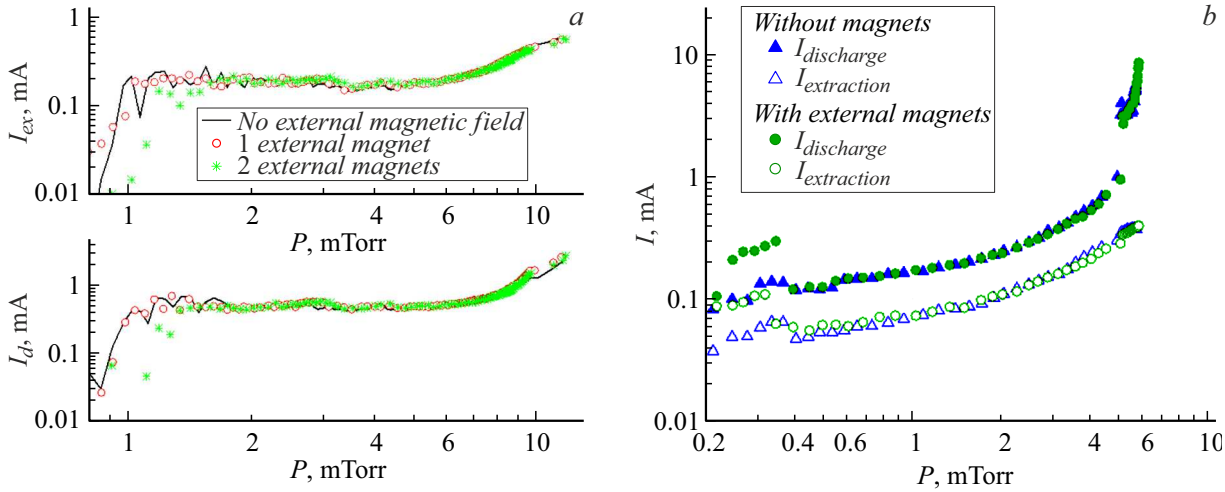

Figure 7. *a* — Magnetic configuration No. 1: dependences of discharge current I_d and extracted current I_{ex} on pressure without and with an external magnetic field; $f = 10$ kHz, $t_{pulse} = 30\,\mu$s. *b* — Magnetic configuration No. 2: dependences of extracted current I_{ex} and discharge current I_d on pressure in the GNT without and with an external magnetic field; $f = 600$ Hz, $t_{pulse} = 200\,\mu$s.

consequently, affect the distribution of magnetic fields in the ion source [22,23,28]. Therefore, one needs to take into account this influence of screens and make appropriate changes to the parameters of the magnetic system (geometry, structures, magnetic materials used) designed for ion sources.

Two types of magnetic shielding for the ion source were examined in the present study. In the first case, the shielding element was the housing (made of structural steel 30ChGSA (14331)) of a well-logging instrument. The thickness of the housing wall was 3 mm, and the external diameter was 43 mm. In the second shielding system design, the ion source was protected with a screen made of electrical steel 1008 (10864) with a wall thickness of 2 mm (the external screen diameter was 40 mm). It should be noted that practical implementation of the proposed options for magnetic PIS shielding requires additional materials research (aimed at selecting proper steels with the specified magnetic and strength properties and resistance to the effects of the external aggressive well environment) if the long-term performance of equipment is to be preserved.

The distribution of magnetic fields in shielded ion sources was modeled in Comsol Mutiphysics. Two magnetic system configurations were chosen from various alternatives based on the results of calculations and experimental measurements of the magnetic field distribution inside the PIS. The first one featured five permanent magnets K30 × 20 × 25 ($B_{z0} = 90$ mT), a 2 mm non-magnetic gap at the anti-cathode, two correcting kovar rings, and a TU housing made of steel 30ChGSA. Four 30 × 20.5 × 25 mm ($B_{z0} = 90$ mT) permanent magnets, a 1 mm non-magnetic gap at the anti-cathode, two correcting kovar rings, a standard TU with an additional magnetic screen made of electrical steel (ES), and an enlarged EU were used in the second configuration.

The $Id(P)$, $I_{ex}(P)$ plots (Fig. 7, *a* — the first configuration; Fig. 7, *b* — the second configuration) make it clear that, regardless of the external magnetic environment, the amplitudes of the extracted and discharge currents remain almost the same within the operating pressure range (3–7 mTorr). At elevated pressures $P > 10$ mTorr, the discharge current amplitudes may differ by 400–500 μA, while the extracted current amplitudes differ by 30–50 μA. The dependences of the delay time on pressure deviate by 0.5–1 μs on average (with or without external magnets); as the pressure increases, the spread of delay times decreases to 0.5 μs. External magnetic disturbances with a transverse direction of magnetization exert the greatest negative effect of transverse field at the cathode and anti-cathode (Fig. 2, options III and IV).

Figure 8 shows the examples of oscilloscope records of the discharge and extracted currents without and with an external magnetic field for two shielded PIS magnetic systems. It can be seen that magnetic shielding establishes the conditions for stable PIS operation within a wide range of time parameters of the pulsed power supply system of the ion source (repetition rate and duration of voltage pulses).

Conclusion

The obtained data provided an insight into the dependences of amplitude parameters and the formation delay of a Penning discharge on the magnitude and configuration of the PIS magnetic field. The parameters of the recommended magnetic field configuration for the GNT PIS were determined based on these data. The results of examination of the operating regimes of ion sources in neutron generators with an external durable housing made of stainless steel 12Kh18N10T demonstrated that the greatest negative effect is exerted by an external magnetic field with a transverse

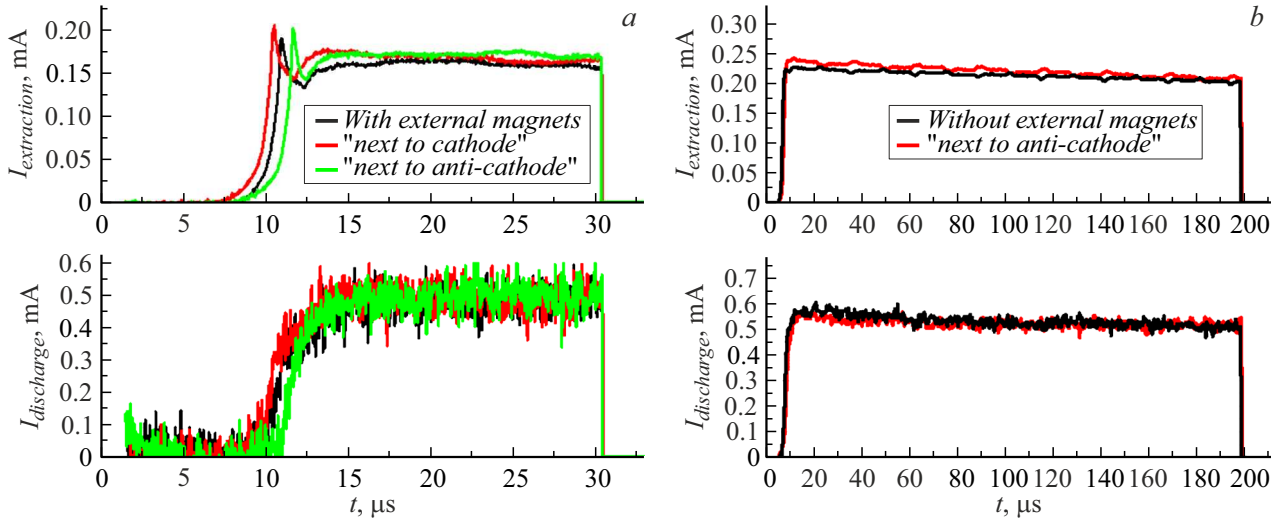

Figure 8. Examples of oscilloscope records of discharge current and extracted current without and with an external magnetic field. *a* — Configuration No. 1, $f = 10$ kHz, $t_{pulse} = 30\,\mu$s; *b* — configuration No. 2, $f = 600$ Hz, $t_{pulse} = 200\,\mu$s.

direction of magnetization. Two GNT magnetic system designs were proposed in order to ensure stable operation of the ion source under external magnetic influences and existing dimensional restrictions: a durable housing of the neutron generator made of structural alloy steel is used as a screen in the first design, and the other is fitted with an additional screen made of electrical steel.

Conflict of interest

The authors declare that they have no conflict of interest.

References

[1] V. Valkovic. *14 MeV Neutrons. Physics and Applications* (CRC Press Taylor& Francis Group, Boca Raton, London, NY., 2016)

[2] E.B. Hooper. *A Review of Reflex and Penning Discharges, in Advances in Electronics and Electron Physics* (Academic Press, NY., 1969), v. 27, p. 295-343.

[3] F.M. Penning, J.H.A. Moubis. Physica, **IV** (11), 71 (1937).

[4] X. Zhou, J. Lu, Y. Liu, X. Ouyang. Nuclear Inst. and Methods in Phys. Research, **A 987**, 164836 (2021). DOI: 10.1016/j.nima.2020.164836

[5] X. Zhou, Y. En, J. Lu, Y. Liu, K. Li, Zh. Lei, Zh. Wang, X. Ouyang. Instrum. Experimental Techniq., **63** (4), 595 (2020). DOI: 10.1134/S002044122004020X;

[6] W. Liu, M. Li, K. Gao, D. Gu. Nuclear Instrum. Methods in Phys. Research, **A768**, 120 (2014). DOI: 10.1016/j.nima.2014.09.052

[7] A. Fathi, S.A.H. Feghhi, S.M. Sadati, E. Ebrahimibasabi. Nuclear Instrum. Methods in Phys. Research, **A 850**, 1 (2017). DOI: 10.1016/j.nima.2017.01.028

[8] N.V. Mamedov, A.S. Rohmanenkov, V.I. Zverev, S.P. Maslennikov, A.A. Solodovnikov, A.A. Uzvolok, D.I. Yurkov. Rev. Sci. Instrum., **90**, 123310 (2019). DOI: 10.1063/1.5127921

[9] F.K. Chen. J. Appl. Phys., **56**, 3191 (1984).

[10] A. Zhang, D. Li, L. Xu, Z. Xiong, J. Zhang, H. Peng, Q. Luo. Phys. Rev. Accelerators and Beams, **25**, 103501 (2022). DOI: 10.1103/PhysRevAccelBeams.25.103501

[11] S. Lei, Q. Mu-Yang, X. Kun-Xiang, Li Ming. Acta Phys. Sinica, **62** (17), 175205 (2013). DOI: 10.7498/aps.62.175205

[12] D.S. Stepanov, A.P. Skripnik, E.Ya. Shkolńikov. Atomic Energy, **128** (5), 318 (2020). DOI: 10.1007/s10512-020-00694-4

[13] E. Burns, G. Bischoff. AIP Conf. Proc., **392**, 1207 (1997). DOI: 10.1063/1.52633

[14] P. Bach, H. Bernardet, V. Stenger. *Operation and life of SODITRON Neutron Tube for Industrial Analysis*, in J.L. Duggan, I.L. Morgan (Eds.). Application of Accelerators in Research and Industry (AIP Press, NY., 1997), p. 905–908.

[15] M. Mahjour-Shafiei, H. Noori, A.H. Ranjbar. Rev. Sci. Instrum., **82**, 113502 (2011). DOI: 10.1063/1.3658201

[16] B.K. Das, A. Shyam. Rev. Scientific Instrum., **79**, 123305 (2008). DOI: 10.1063/1.3054268

[17] A. Sy, Q. Ji, A. Persaud, O. Waldmann, T. Schenkel. Rev. Scientific Instrum., **83**, 02B309 (2012). DOI: 10.1063/1.3670744

[18] M.S. Lobov, I.M. Mamedov, N.V. Mamedov, A.Yu. Presniakov, V.I. Zverev, D.I. Iurkov. Tech. Phys., **68** (6), 726 (2023). DOI: 10.21883/JTF.2023.06.55602.16-23

[19] A.D. Liberman, F.K. Chen. Proc. SPIE, **2339**, 188 (1995).

[20] Yu.N. Barmakov, E.P. Bogolyubov, V.V. Miller, Yu.G. Polkanov, V.I. Ryzhkov, I.A. Titov. Karotazhnik, **10**–**11**, 175 (2006) (in Russian).

[21] D.I. Yurkov, E.P. Bogolyubov, V.V. Miller, S.I. Kopylov, G.G. Yatsenko, F.Kh. Enikeeva, L.A. Magadova, Z.R. Davletov, V.Yu. Solokhin, A.F. Shaimardarov. Karotazhnik, **9**, 77 (2013) (in Russian).

[22] R.S. Rachkov, A.Yu. Presnyakov, D.I. Yurkov. At. Energy, **126** (6), 383 (2019).

[23] R.S. Rachkov, A.Yu. Presnyakov. Yad. Fiz. Inzh., **7** (2), 162 (2016) (in Russian).

[24] G.V. Smirnitskaya, Nguyen Huu Ti. Vestn. Mosk. Gos. Univ., **1**, 3 (1969) (in Russian).
[25] E.M. Reikhrudel', G.V. Smirnitskaya, G.A. Egiazaryan. Zh. Tekh. Fiz., **43**, 130 (1973) (in Russian).
[26] E.M. Reikhrudel', G.V. Smirnitskaya, Nguyen Huu Ti. Zh. Tekh. Fiz., **39**, 1052 (1969) (in Russian).
[27] Yu.E. Kreindel'. *Plazmennye istochniki elektronov* (Atomizdat, M., 1977), p. 144 (in Russian).
[28] N.V. Mamedov, S.P. Maslennikov, A.A. Solodovnikov, D.I. Yurkov. Plasma Phys. Reports, **46** (2), 217 (2020). DOI: 10.1134/S1063780X20020063
[29] N.V. Mamedov, A.V. Gubarev, V.I. Zverev, S.P. Maslennikov, A.A. Solodovnikov, A.A. Uzvolok, D.I. Yurkov. Plasma Sources Sci. Technol., **29**, 025001 (2020). DOI: 10.1088/1361-6595/ab6758
[30] S.P. Maslennikov, I.M. Mamedov. At. Energy, **133** (1), 54 (2022).
[31] N.V. Mamedov, A.S. Rohmanenkov, A.A. Solodovnikov. J. Phys. Conf. Ser., **2064**, Art.N. 012039 (2021). DOI: 10/1088/1742-6596/2064/1/012039
[32] A.V. Sy. *Advanced Penning-Type Source Development and Passive Beam Focusing Techniques for an Associated Particle Imaging Neutron Generator with Enhanced Spatial Resolution* (Diss. California, 2013)
[33] E.T. Kucherenko, V.A. Saenko. Zh. Tekh. Fiz., **37** (1), 112 (1967) (in Russian).
[34] N.V. Mamedov, S.P. Maslennikov, Yu.K. Presnyakov, A.A. Solodovnikov, D.I. Yurkov. Tech. Phys., **64** (9), 1290 (2019). DOI: 10.1134/S1063784219090081
[35] N.V. Mamedov, A.S. Rokhmanenkov, I.A. Kan'shin, S.P. Maslennikov, M.S. Lobov, A.A. Solodovnikov. Mater. Technol. Des., **5** (4(14)), 42 (2023) (in Russian). DOI: 10.54708/26587572_2023_541442
[36] N. Mamedov, D. Prokhorovich, I. Kanshin, A. Solodovnikov, D. Kolodko, I. Sorokin. AIP Conf. Proceed., **2011**, 080006 (2018). DOI: 10.1063/1.5053361
[37] A.N. Dolgov, V.G. Markov, A.A. Okulov, D.E. Prokhorovich, A.G. Sadilkin, D.I. Yurkov, I.V. Vizgalov, V.I. Rashchikov, N.V. Mamedov, D.V. Kolodko. Usp. Prikl. Fiz., **2** (3), 267 (2014) (in Russian).
[38] I.A. Kanshin, A.A. Solodovnikov. Instrum. Experimental Techniq., **63** (3), 315 (2020). DOI: 10.1134/S0020441220030112
[39] N. Mamedov, D. Prokhorovich, D. Yurkov, I. Kanshin, A. Solodovnikov, D. Kolodko, I. Sorokin. Instrum. Experimental Techniq., **61**, 530 (2018). DOI: 10.1134/S0020441218030223

Translated by D.Safin